ELSEVIER

Journal of Alloys and Compounds 217 (1995) 137–147

Journal of ALLOYS AND COMPOUNDS

Solid state properties of group IVb carbonitrides

W. Lengauer[a,*], S. Binder[a], K. Aigner[a], P. Ettmayer[a], A. Guillou[b], J. Debuigne[b], G. Groboth[c]

[a]*Institute for Chemical Technology of Inorganic Materials, Vienna University of Technology, Getreidemarkt 9, A-1060 Vienna, Austria*
[b]*Laboratoire de Métallurgie et Physico-Chimie des Matériaux, CSIM, URA CNRS No. 1495, INSA Rennes, 20 Avenue des Buttes de Coësmes, F-35043 Rennes, France*
[c]*Austrian Research Centre Seibersdorf, A-2444 Seibersdorf, Austria*

Received 2 June 1994

Abstract

Technically relevant solid state properties of the hot-pressed group IVb carbonitrides $Ti(C_xN_{1-x})_{\approx 1.00}$, $Ti(C_xN_{1-x})_{0.82}$, $Zr(C_xN_{1-x})_{\approx 1.00}$ and $Hf(C_xN_{1-x})_{\approx 1.00}$, such as microhardnesses, electrical conductivities, heat conductivities (from specific heats and temperature diffusivities) and optical reflectances (visible region), were measured as functions of the [C]/([C]+[N]) ratio. Generally the electrical conductivities, heat conductivities and molar heat values increase with increasing nitrogen content whereas the microhardnesses decrease. In samples of the series $Ti(C_xN_{1-x})_{0.82}$ a discontinuity in the C_p vs. T curves could be detected at 700–820 °C depending on the [C]/([C]+[N]) ratio, indicative of a phase transition. The colour of the IVb carbonitrides changes from yellow through violet to grey with increasing [C]/([C]+[N]) ratio. The extension of the coloured region is greater the higher the atomic number of the metal. A variety of these properties of IVb carbonitrides were measured for the first time. A literature review is presented.

Keywords: Solid state properties; IVB carbonitrides; Phase transitions; High-melting compounds

1. Introduction

$Ti(C_xN_{1-x})_{1-y}$, $Zr(C_xN_{1-x})_{1-y}$ and $Hf(C_xN_{1-x})_{1-y}$ are hard, high melting compounds. Especially $Ti(C_xN_{1-x})_{1-y}$ has found application in carbonitride hard metals, the so-called cermets, where it constitutes the hard phase and is bonded with Ni and/or Co to form a tough and wear-resistant hard metal [1]. In addition, $Ti(C_xN_{1-x})$ has found widespread application as a coating for hard metal cutting tips in the form of chemical vapour deposition (CVD) layers. Modern coated hard metals generally feature multilayer coatings which often change gradually from a nitrogen-rich composition on the top to a nitrogen-poor composition on the layer adjacent to the substrate in order to meet such requirements as good adherence with the hard metal and reaction resistance at the surface because of tool–workpiece interaction. $Zr(C_xN_{1-x})_{1-y}$ and $Hf(C_xN_{1-x})_{1-y}$ are only rarely used in technical applications but have in principle the same favourable properties as $Ti(C_xN_{1-x})_{1-y}$ and could be used accordingly.

A number of studies have been performed in order to assess various solid state properties of carbides, nitrides and carbonitrides of the group IVb metals, the last of which are reviewed here. (For many of the properties of binary carbides and nitrides as a function of the non-metal/metal ratio the reader is referred to well-known older compilations [2,3] as well as to the latest reviews and results [4–6].) Isothermal sections of the phase equilibria in the systems Ti–C–N, Zr–C–N and Hf–C–N have recently been investigated [7].

1.1. Review of literature data

Literature data are included whenever necessary in the graphical representations of Section 3.

1.1.1. Hardness

Some Vickers microhardness data of IVb carbonitrides have been reported for $Ti(C_xN_{1-x})_{1-y}$ [8–10], $Zr(C_xN_{1-x})_{1-y}$ and $Hf(C_xN_{1-x})_{1-y}$ [10] which scatter by a factor of up to 2. For $Ti(C_xN_{1-x})_{1-y}$ some authors have found positive deviations from the additivity rule [8], i.e. $H_V(Ti(C_xN_{1-x})) > xH_V(TiC) + (1-x)H_V(TiN)$,

*Corresponding author.

SSDI 0925-8388(94)01315-9

whereas others have observed the opposite behaviour [9].

1.1.2. Electrical conductivity

The electrical conductivity of $Ti(C, N)_{1.00}$ has been found to follow the additivity rule between TiC and TiN, i.e. $\sigma(Ti(C_xN_{1-x}))=x\sigma(TiC)+(1-x)\sigma(TiN)$, as stated by Barbier and Thevenot [11] but without giving the detailed data. The electrical conductivity of $Hf(C_xN_{1-x})_{1-y}$ was investigated for two different ([C]+[N])/[Hf]) ratios ($1-y\approx1.00$ and 0.83) at room temperature and 1200 K [12]. In the stoichiometric hafnium carbonitrides a distinct deviation from a linear behaviour was found.

1.1.3. Heat conductivity

Taylor [13] was the first to observe that the heat conductivity of TiC increases with increasing temperature. This was also found for other carbides and nitrides, e.g. TiN and ZrC [14,15], and is explained by the low electronic contribution to the heat conductivity, k_e, at room and moderately elevated temperatures to the total heat conductivity k_t. The heat conductivity is the sum of the electronic and phonon conductivities, i.e. $k_t=k_p+k_e$; k_p remains approximately constant at $T>300$ K and k_e increases, while in metals k_e is approximately constant and k_p is proportional to $1/T$. The result is a deviation from the Wiedemann–Franz law $k_e=L_o\sigma T$, where σ is the electrical conductivity at temperature T and L_o is the classical Lorenz number which is constant for metals to a first approximation. At ambient and moderate temperatures L_o of the carbides and nitrides is much higher than that of metals and approaches approximately the value of pure metals at high temperatures.

A variety of effects have been proposed as causes for the peculiar k_t vs. T behaviour [16]. Phonon scattering due to non-metal vacancies was thought to be the most important one. In addition, ambipolar diffusion – a simultaneous and independent diffusion of both electrons and holes in a temperature gradient, thereby transporting thermal energy as long as they do not annihilate each other – was regarded as being responsible for this behaviour at high temperatures [17]. Although quite a number of investigations have been published on the heat conductivities of transition metal carbides and nitrides, the samples on which these properties were measured were sometimes insufficiently characterized with respect to composition and porosity.

1.1.4. Heat capacity

Turchanin and coworkers [18–20] measured the heat capacities of titanium and zirconium carbonitrides. In one study [18] on titanium carbonitrides they stated a distinct minimum in C_p for a composition $TiC_{0.66}N_{0.28}$ (pure TiC and TiN were not investigated in this study) at $T=500$, 800 and 900 K and gave a function of C_p vs. composition and temperature, while in another study [19] a linear behaviour was reported. No heat capacity data on hafnium carbonitrides could be found in the literature.

1.1.5. Colour

The binary nitrides TiN, ZrN and HfN have a distinct yellow colour which is strongly influenced by the metal/nitrogen ratio [21–26]. A reflectance minimum in the blue region of the spectrum of these compounds occurs, giving rise to their yellow appearance. Many of the reported studies were performed on thin films where the characterization of the composition is difficult and prone to error. Some nitrogen-rich IVb carbonitrides are coloured too, which has attracted a study on the spectral reflectance as a function of the [C]/[N] ratio for $Ti(C_xN_{1-x})_{1-y}$ and $Zr(C_xN_{1-x})_{1-y}$ [26]. With increasing C content the colour disappears and the carbonitrides become dark grey.

1.1.6. Resume of literature survey

The published data on the IVb carbonitrides generally suffer from poorly characterized samples with respect to gross compositions of carbon and nitrogen and minor contaminants such as oxygen as well as to porosity. This is reflected in the sometimes considerable scatter in data for nominally identical compositions. While data for the binary carbides and nitrides have frequently been collected and compiled, data for carbonitrides are scarce. Because of these deficiencies, we carried out a systematic study of two series of titanium carbonitrides, $Ti(C_xN_{1-x})_{\approx1.0}$ and $Ti(C_xN_{1-x})_{0.82}$, as well as of the carbonitride series $Zr(C_xN_{1-x})_{\approx1.00}$ and $Hf(C_xN_{1-x})_{\approx1.0}$ using well-characterized sample material throughout.

2. Experimental details

2.1. Preparation of samples

Carbide, nitride and carbonitride powders as described in Table 1 were mixed in a planetary ball mill with cyclohexane as a milling aid, dried and hot pressed to nearly full density in a graphite die at temperatures up to about 2500 °C at a pressure of 55 MPa under an Ar atmosphere with a ramp time of 10 min. Samples of 15 mm diameter and about 8 mm height were prepared. Layers of graphite foil and Zr foil were placed between the powder and the graphite die. The graphite foil prevented sticking between the die and the sample, which otherwise led to cracking of the samples. The Zr foil was carburized during the hot-pressing cycle and served as a getter as well as a diffusion barrier.

Table 1
Specifications of starting powders (H.C. Starck, Germany)

Powder	Metal content (wt.%)	C total (C free) (wt.%)	N (wt.%)	O (wt.%)	Metal impurities (wt.%)	Grain size FSSS[a] (μm)
TiC A	–	19.57 (0.17)	1.1 ppm	1.9 ppm	–	2.4
TiC	–	19.28 (0.17)	0.46	6.4 ppm	–	1.3
TiN A	77	0.005 (–)	21.9	0.35	<0.15	4.8
TiN B	77	0.07 (–)	22.3	0.9	<0.15	1.3
ZrC	87.0 Zr, 1.9 Hf	11.34 (0.24)	0.355	0.199	0.015	3.9
ZrN	>86.7 Zr+Hf	0.73 (–)	11.2	2.1	–	4.3
HfC	93.12 Hf, <0.1 Zr	6.06 (0.06)	0.278	0.033	0.404	6.3
HfN	90.04 Hf, 2.06 Zr	0.09 (–)	7.09	0.366	0.05	4
Ti(C, N) 30/70	>76	6.6 (–)	14.3	0.45	<0.15	5
Ti(C, N) 50/50	>76	9.7 (–)	11.1	0.27	<0.15	3.3
Ti(C, N) 70/30	>76	13.25 (–)	6.8	0.2	<0.15	4.1

[a]Fisher subsieve sizer.

2.2. Characterization

For phase analysis a standard powder diffractometer with Cu Kα radiation, a graphite monochromator and a rotating sample holder was used. High purity silicon served as a standard for goniometer calibration.

Chemical analyses for nitrogen and carbon were done by Dumas gas chromatography (GC) on a Carlo ERBA CHN 1108 analyser. The sample was placed in an Sn crucible, mixed with V_2O_5 and combusted in an He–O_2 atmosphere. The peak areas of CO_2 and N_2 as detected by the GC column were calibrated against organic standards of well-known composition [27].

Metallographic analysis was performed by grinding the samples first with a diamond disc, then by polishing with diamond paste and finally by SiO_2 suspension.

Reflectance measurements were performed with a photometer of our own design and using well-polished hot-pressed samples of about 14 mm diameter. The incident angle of light was 45° and the take-off angle 135° from the surface. Absolute intensity data agreed within better than 10% when repeated on the same sample.

Heat capacity measurements were done with a Netzsch 404 differential scanning calorimeter under high purity Ar at a heating rate of 20 K min^{-1}. The samples were cylindrical plates 5 mm in diameter and 1 mm thick. A sapphire standard was used. The errors of the measurements are within $\pm 1\%$.

Temperature conductivity measurements were performed by the laser flash technique using cylindrical specimens 10 mm in diameter and 1 mm thick cut and ground from the hot-pressed material. The sample was placed on three thin Al_2O_3 supports to minimize the heat loss by conduction and heated in vacuum by means of a resistance furnace. The front side of each sample was subjected to an Nd glass laser flash with an energy of 40 J at a pulse duration of 0.5 ms. The temperature on the rear side of the sample was determined pyrometrically as a function of time. By applying the laws governing diffusion, it is possible to determine the temperature conductivity as [28]

$$\alpha = \frac{0.1388h^2}{t_{1/2}} \quad (1)$$

where h is the height (thickness) of the sample (around 1 mm) and $t_{1/2}$ is the time elapsed between the moment of the flash and the time when the rear side reached 50% of its vertex temperature. The heat loss during the measurements, which introduced some error, is minimized by the small alumina tips on which the sample is placed and the introduction of radiation shields. The remaining error due to radiation loss was corrected according to Clark and Taylor [29]. The measurements were calibrated against a steel standard and were accurate to within $\pm 4\%$.

Temperature conductivity, specific heat and density measurements were combined to give the heat conductivity according to the formula

$$k_t(T) = \alpha(T)C_p(T)\rho(298) \quad (2)$$

where $\alpha(T)$ is the temperature diffusivity (Eq. (1)), $C_p(T)$ is the specific heat and $\rho(298)$ is the density at room temperature. The last value was not corrected for thermal expansion to yield the high temperature density owing to its small influence (maximum 3% at the highest investigation temperatures [30]) relative to the measurement error (maximum 8%). For calculating $k_t(T)$ in Eq. (2), the $\alpha(T)$ values were fitted by polynomial equations. The C_p values of some intermediate carbonitrides were calculated by linear interpolation of the experimental data.

Electrical resistance measurements at room temperature were performed by means of an inductive eddy current principle (Förster, Reutlingen, Germany). The readings were calibrated against standards of well-

defined alloys. Polished as well as ground samples about 14 mm in diameter and 10 mm thick were used.

Vickers microhardness measurements were made on polished samples with a load of 0.98 N.

3. Results and discussion

Table 2 gives the results of the chemical characterization as well as the densities and porosities of the samples. It can be seen that the porosity is generally below about 5% and that it tends to increase with increasing nitrogen content of the sample. Obviously the sintering behaviour is not as favourable for nitrogen-rich as for carbon-rich samples. This is probably due to a small oxygen contamination present in the starting powders. The higher the carbon content, the more easily chemisorbed oxygen will be reduced by formation of CO upon hot pressing. Hot isostatic pressing at 2100 °C and 200 MPa for 90 min of the hot-pressed samples did not yield significantly higher densities. Apparently the temperature was too low to induce plastic flow in the carbonitrides.

The measured values of the electrical conductivities and temperature diffusivities were corrected for the porosity by utilizing the equations derived by Ondracek [31] for field properties of porous materials under the assumption that the pores are spherical, dispersed equidistantly within the carbonitride matrix, not interconnected and do not exceed 10 vol.%:

$$x_{corr} = x_{obs} P^{-3/2} \quad (3)$$

where x_{corr} is the corrected value, x_{obs} is the measured value and P is the ratio of measured density to X-ray density.

3.1. Lattice parameters

Figs. 1a–1d show the lattice parameters of the four series of carbonitrides investigated. The α_1–α_2 splitting of the diffraction lines was excellent, indicating a good homogeneity of the samples. It can be seen from Figs. 1a–1d that the lattice parameters are linear functions of composition between the nitrides and the corresponding carbides in each case.

3.2. Hardness

Fig. 2 shows the Vickers microhardness $H_V(0.1)$ for the two titanium carbonitride series (Fig. 2a) as well as for $Zr(C_xN_{1-x})_{1-y}$ and $Hf(C_xN_{1-x})_{1-y}$ (Fig. 2b) as a function of the [C]/([C]+[N]) ratio. The carbides are harder than the corresponding nitrides. The data of Bogomolov et al. [8] for titanium carbonitrides (no

Table 2
General characterization of hot-pressed samples. Samples with * were not analysed

Sample	C (wt.%)	N (wt.%)	C (at.%)	N (at.%)	Me (at.%)	[C]/([C]+[N])	Density (g cm^{-3})	Porosity (%)
Ti 550	19.27±0.09	0.22±0.06	48.6	0.5	50.9	0.99	4.87	0.9
Ti 541	15.37±0.05	4.67±0.07	39.0	10.1	50.9	0.79	4.95	1.0
Ti 532	11.58±0.20	9.14±0.27	29.5	19.9	50.6	0.60	5.01	1.8
Ti 523	7.76±0.05	13.64±0.19	19.8	29.9	50.3	0.40	5.03	3.3
Ti 514	3.94±0.01	22.19±0.21	10.3	38.1	51.6	0.21	5.11	3.5
Ti 505	0.20±0.05	22.19±0.21	0.5	49.2	50.3	0.01	5.16	4.3
Ti 450	*	*	45.0	0.0	55.0	1.00	4.70	0.7
Ti 369	13.25±0.06	3.97±0.03	35.4	9.1	55.5	0.80	4.78	0.9
Ti 2718	10.03±0.03	7.79±0.04	26.9	17.9	55.2	0.60	4.86	1.1
Ti 1827	*	*	18.0	27.0	55.0	0.40	4.94	1.4
Ti 936	*	*	9.0	36.0	55.0	0.20	5.02	1.6
Ti 045	*	*	0.0	45.0	55.0	0.00	5.11	1.8
Zr 550	11.39±0.01	0.43±0.05	48.7	1.6	49.1	0.96	6.66	1.0
Zr 541	9.21±0.03	2.42±0.01	39.9	9.0	49.8	0.79	6.58	3.8
Zr 532	7.10±0.02	4.49±0.02	30.9	16.8	49.7	0.61	6.65	4.5
Zr 523	5.03±0.02	6.65±0.03	21.9	24.8	49.4	0.43	6.92	2.1
Zr 514	2.90±0.03	8.94±0.02	12.6	33.2	49.0	0.25	7.06	1.8
Zr 505	1.33±0.01	10.67±0.03	5.7	39.5	49.4	0.11	7.14	2.2
Hf 550	6.09±0.01	0.32±0.01	48.1	2.1	49.8	0.96	12.52	1.2
Hf 541	4.90±0.01	1.66±0.01	38.7	11.3	50.0	0.78	12.37	4.1
Hf 532	3.68±0.01	3.01±0.01	29.3	20.5	50.3	0.59	12.44	5.2
Hf 523	2.513±0.01	4.37±0.01	19.9	29.8	50.3	0.40	12.64	5.3
Hf 514	1.333±0.01	5.68±0.04	10.6	38.8	50.6	0.21	13.02	4.1
Hf 505	1.296±0.01	6.95±0.02	2.3	47.2	48.5	0.05	13.08	5.2

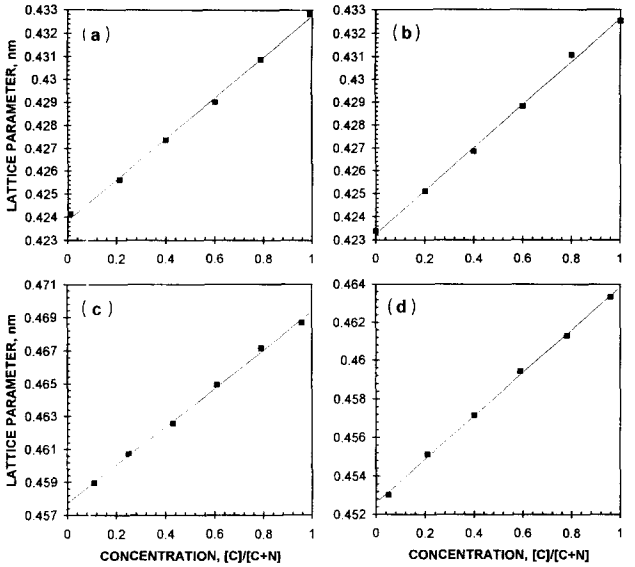

Fig. 1. Lattice parameters of IVb carbonitrides as a function of [C]/([C]+[N]) ratio. a, $Ti(C_xN_{1-x})$; b, $Ti(C_xN_{1-x})_{0.82}$; c, $Zr(C_xN_{1-x})$; d, $Hf(C_xN_{1-x})$.

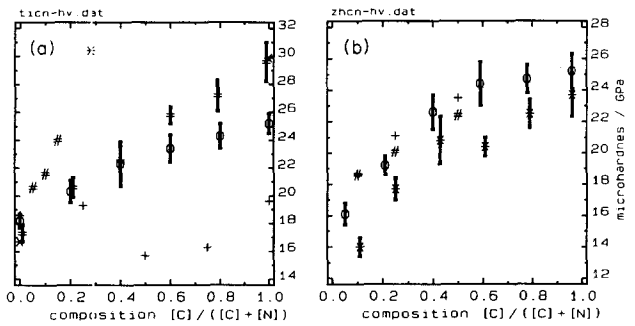

Fig. 2. Vickers microhardness values of IVb carbonitrides at room temperature. Load 0.98 N. a: =, $Ti(C_xN_{1-x})_{1.00}$; O, $Ti(C_xN_{1-x})_{0.82}$; *, Ref. [8], load ?, one data point for [C]/([C]+[N])=0.57 at 38.3 GPa not shown; +, Ref. [9], load 0.98 N; #, Ref. [2], load 0.49 N. b: *, $Zr(C_xN_{1-x})_{1.00}$; #, Ref. [2], load 0.49 N; O, $Hf(C_xN_{1-x})_{1.00}$; +, Ref. [2], load 0.49 N.

load given) show a large deviation from our values, except for the boundary compounds TiN and TiC, with a very high maximum at [C]/([C]+[N])=0.57 of 38.3 GPa (not shown in Fig. 2a). For $Ti(C_xN_{1-x})_{1-y}$ a crossover of the function hardness vs. composition of stoichiometric and substoichiometric samples could be observed, in full agreement with the fact that the hardness increases with the [C]/[Ti] ratio in TiC_{1-x} [32,33] but decreases with the [N]/[Ti] ratio in TiN_{1-x} [34]. Whether a positive deviation from the additivity rule, i.e. $H_V(Ti(C_xN_{1-x})_{1-y}) > xH_V(TiC)+(1-x)H_V(TiN)$, can really be observed in stoichiometric titanium carbonitrides has yet to be substantiated, while for the substoichiometric series this deviation is more pronounced. The positive deviation of microhardness as a function of [C]/([C]+[N]) appears to be more pronounced for $Zr(C_xN_{1-x})_{1-y}$ and $Hf(C_xN_{1-x})_{1-y}$ as can be seen from Fig. 2b.

3.3. Electrical conductivity

The electrical conductivities are shown in Fig. 3. All three stoichiometric carbonitrides appear to behave very similarly. The substoichiometric $Ti(C_xN_{1-x})_{0.82}$ could not be measured because the conductivity was below the range of the instrument. The electrical conductivities increase with increasing nitrogen content. The data were fitted to the polynomial equation

$$\sigma = A + B\frac{[C]}{[C]+[N]} + C\left(\frac{[C]}{[C]+[N]}\right)^2 + D\left(\frac{[C]}{[C]+[N]}\right)^3 \quad (10^6\ \Omega^{-1}\ cm^{-1}) \tag{4}$$

and the coefficients A, B, C and D are given in Table 3.

The present findings for $Ti(C_xN_{1-x})_{1.00}$ are not entirely in agreement with the results of Barbier and Thevenot [11], who reported a linear function. Also, the values of Schulz [12] for $Hf(C_xN_{1-x})$ are in poor agreement with the present data.

Even if the Wiedemann–Franz law cannot be applied to the carbonitrides of the IVb transition metals, the

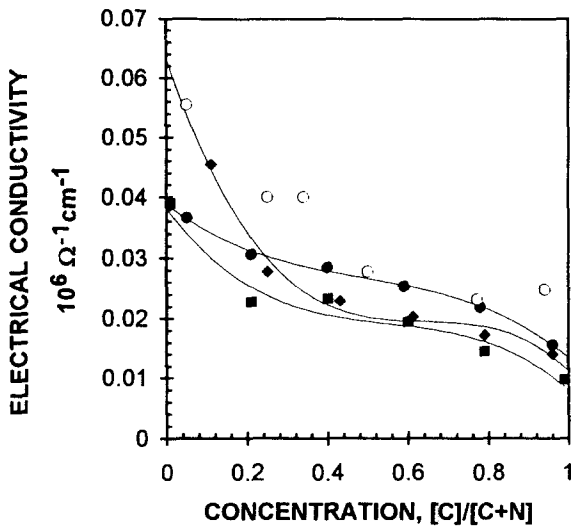

Fig. 3. Electrical conductivities of stoichiometric IVb carbonitrides at room temperature as a function of [C]/([C]+[N]) ratio fitted by polynomials. The coefficients for the polynomials are given in Table 3. ■, $Ti(C_xN_{1-x})$; ◆, $Zr(C_xN_{1-x})$; ●, $Hf(C_xN_{1-x})$; O, $Hf(C_xN_{1-x})$ [12].

Table 3
Coefficients of the polynomial $\sigma = A + B[C]/([C]+[N]) + C\{[C]/([C]+[N])\}^2 + D\{[C]/([C]+[N])\}^3$ for the electrical conductivity as a function of the [C]/([C]+[N]) ratio (see Fig. 3)

Compound	A	B	C	D
$Ti(C_xN_{1-x})$	0.0389	−0.0903	0.1467	−0.0868
$Zr(C_xN_{1-x})$	0.0630	−0.1999	0.3091	−0.1611
$Hf(C_xN_{1-x})$	0.0387	−0.0505	0.0800	−0.0548

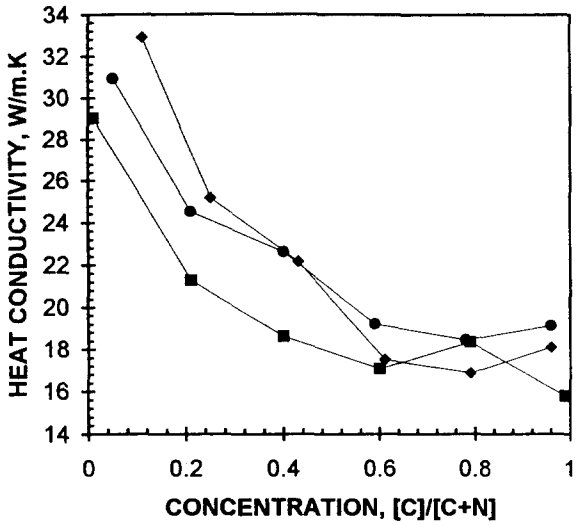

Fig. 4. Heat conductivities at 50 °C of stoichiometric carbonitrides as a function of [C]/([C]+[N]) ratio. The heat conductivity behaves similarly to the electrical conductivity (see Fig. 3). ■, $Ti(C_xN_{1-x})$; ◆, $Zr(C_xN_{1-x})$; ●, $Hf(C_xN_{1-x})$.

similar behaviours of electrical and temperature conductivities as functions of the [C]/([C]+[N]) ratio at stoichiometric compositions and at 50 °C (lowest investigation temperature) are quite obvious if Figs. 3 and 4 are compared.

3.4. Molar heat capacity

The molar heat capacities of IVb carbides and nitrides are shown in Figs. 5a–5c together with literature data. Generally, with increasing temperature the molar heat approaches the theoretical value of 52 J mol^{-1} (Dulong–Petit rule) or even exceeds it. Nitrides show a larger heat capacity than carbides and the carbonitrides have intermediate values. The data points for each composition were fitted to the equation

$$C_p(T) = A + BT + CT^2 + DT^{-2} \quad (\text{J mol}^{-1}\ \text{K}^{-1}) \qquad (5)$$

where T is the absolute temperature. The coefficients of the polynomials are given in Table 4.

The values of the present study for TiC are slightly lower than those reported in the literature [35,36] (Fig. 5a). For TiN the agreement with literature data is closer [35], except for high temperatures. It cannot be entirely precluded that at high temperature, even in high purity argon, a slight oxidation of the sample took place and therefore the heat of reaction results in low values for the specific heat capacity. The values of Turchanin [37] for TiC (not shown in Fig. 5b) are only slightly lower than ours. For ZrC the values in the literature scatter widely [38–40] (Fig. 5b). The best agreement with our values is found for the data of Hultgren et al. [40] at temperatures lower than about 700 K, whereas our ZrN values are somewhat higher than those determined by Coughlin and King [41]. Quite

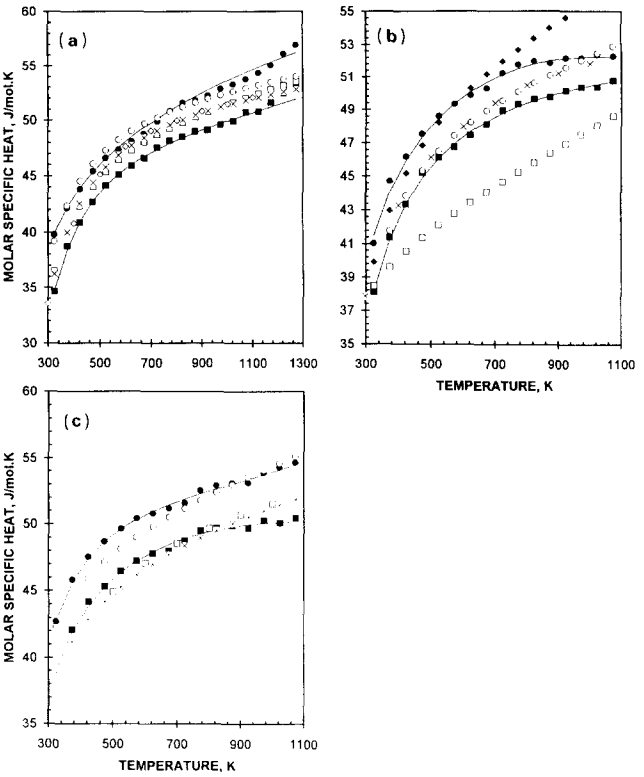

Fig. 5. Molar heat capacities of IVb carbides and nitrides as a function of temperature together with literature data. The heat capacities of the corresponding stoichiometric carbonitrides as a function of temperature were found to lie in between the two curves (linear dependence on [C]/([C]+[N]) ratio). They were not introduced in this graph because of legibility, but are contained in numerical form in Table 4. For the substoichiometric titanium carbonitrides see also Fig. 8. a: ■, TiC; ●, TiN; ◇, TiC [35]; □, TiC [36]; ×, TiC [39]; ○, TiN [36,39,40]. b: ■, ZrC; ●, ZrN; □, ZrC [38]; ◇, ZrC [39]; ×, ZrC [40]; ○, ZrN [41]. c: ■, HfC; ●, HfN; □, HfC [39]; ×, HfC [40]; ○, HfN [39,40].

Table 4
Coefficients of the polynomial $C_p(T) = A + BT + CT^2 + DT^{-2}$ for the C_p data fit for the stoichiometric samples (see Figs. 5a–5c). The C_p data of $Ti(C_xN_{1-x})_{0.82}$ were not fitted owing to the discontinuity

[C]/([C]+[N])	A	$B\times10^3$	$C\times10^6$	$D/10^5$
$Ti(C_xN_{1-x})$				
0.01	41.45	16.26	−3.884	−6.734
0.60	42.30	20.63	−10.560	−11.155
0.99	48.38	1.302	1.742	−14.834
$Zr(C_xN_{1-x})$				
0.11	44.87	18.0	−9.752	−8.554
0.25	47.11	11.9	−6.029	−9.503
0.96	48.18	5.35	−1.851	−12.021
$Hf(C_xN_{1-x})$				
0.05	54.39	−4.50	4.616	−11.454
0.40	45.64	13.51	−6.459	−9.358
0.59	45.70	13.20	−6.070	−8.523
0.96	48.19	6.22	−3.142	−11.320

good agreement could be found for both HfC and HfN with literature values [39,40] (Fig. 5c).

Within the accuracy of the results the present findings indicate a linear dependence for C_p as a function of the [C]/([C]+[N]) ratio for titanium carbonitrides. Turchanin et al. [18] found a minimum in C_p at [C]/([C]+[N])=0.70 for a near-stoichiometric series of titanium carbonitrides. However, in another study Turchanin et al. [19] reported a linear behaviour for C_p as a function of composition and gave higher values. The values are compared in Fig. 6 for selected temperatures. The heat capacity data of the zirconium carbonitrides agree quite well with the values of Turchanin and Babenko [20], as can be seen from Fig. 7.

An interesting C_p vs. T behaviour was observed for the $Ti(C_xN_{1-x})_{0.82}$ series. A distinct and reproducible

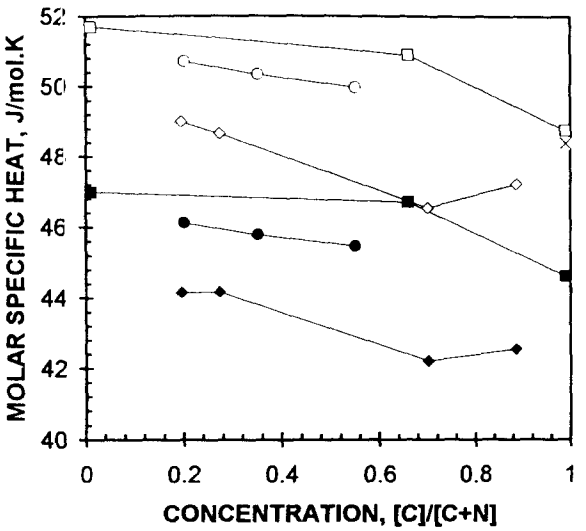

Fig. 6. Comparison of heat capacity data for titanium carbonitrides of Turchanin and coworkers [18,19] with our values. 500K: ■, Ti(C, N); ◆, Ti(C, N) [18]; ●, Ti(C, N) [19]. 800 K: □, Ti(C, N); ◇, Ti(C, N) [18]; ○, Ti(C, N) [19]; ×, TiC [37].

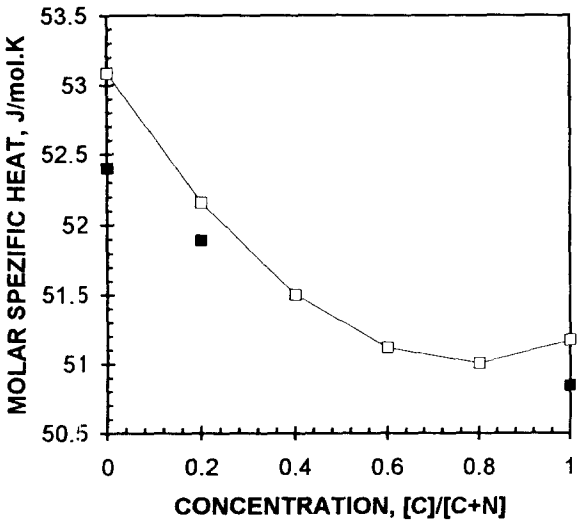

Fig. 7. Comparison of heat capacity data for zirconium carbonitrides at 1100 K of Turchanin and Babenko [20] (□) with our values (■).

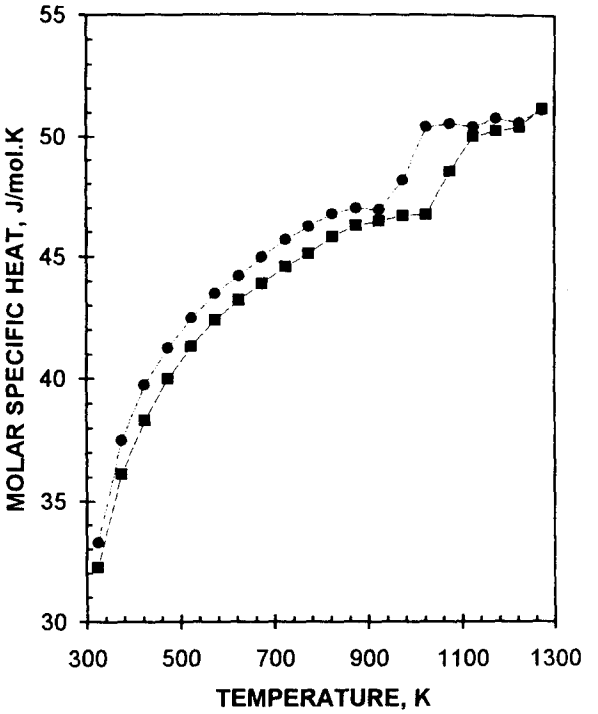

Fig. 8. Heat capacity of $TiC_{0.82}$ and $TiN_{0.82}$ upon heating. Note the discontinuity at 1068 K for $TiC_{0.82}$ (■) and at 973 K for $TiN_{0.82}$ (●).

endothermic C_p discontinuity could be detected, which is also present in the binary compounds TiN and TiC (Fig. 8) upon heating. Upon cooling, a reversible nature of the C_p behaviour was observed but shifted towards slightly lower temperatures, which is evidence of a phase transition. Fig. 9 shows the transition temperature T_c as a function of the [C]/([C]+[N]) ratio (where ([C]+[N])/[Ti] is fixed at 0.82). It is seen that the transition temperature increases with increasing nitrogen content.

Standard X-ray powder diffraction measurements of samples quenched or cooled from temperatures both above and below the C_p discontinuity did not reveal any deviations with respect to the line pattern or the lattice parameters. If the discontinuities can be considered to stem from an ordered phase, it must be a different phase from the one described by Arbuzov et al. [42], who, upon investigation of the Ti–C–N system at 500 °C, described an ordered titanium carbonitride phase which forms at $T<1000$ °C and reaches from the Ti–C boundary system at about 38–40 at.% C into the ternary with a minimum [TiC]/[TiN] ratio of about 0.70. Furthermore, it is also different from the $\delta'-TiN_{1-x}$ phase [43–45] which exists in the Ti–N boundary system and can be obtained by heat treatment of $\delta-TiN_{1-x}$ followed by cooling to room temperature.

3.5. Temperature diffusivity

The temperature diffusivity measurements were made on the same samples as for the molar heat capacity

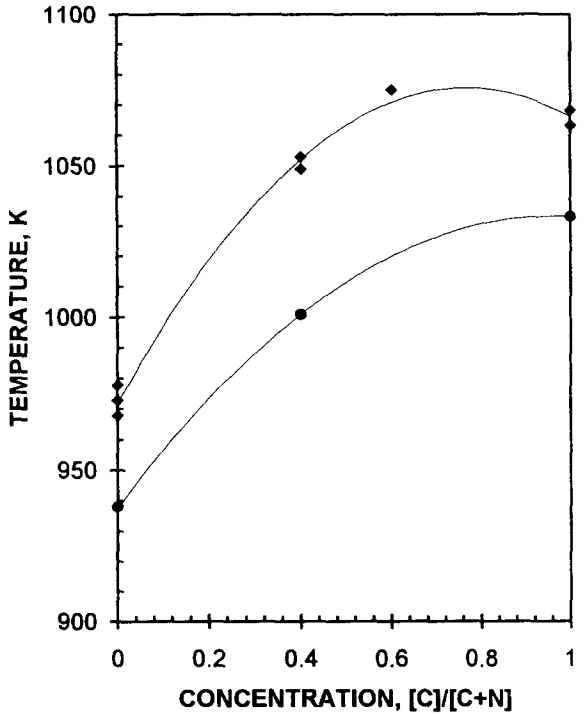

Fig. 9. Phase transition temperatures T_c (midpoint of transition) of $Ti(C_xN_{1-x})_{0.82}$ as a function of [C]/([C]+[N]) ratio as reflected in C_p measurements. Upper curve: ♦, heating. Lower curve: ●, cooling.

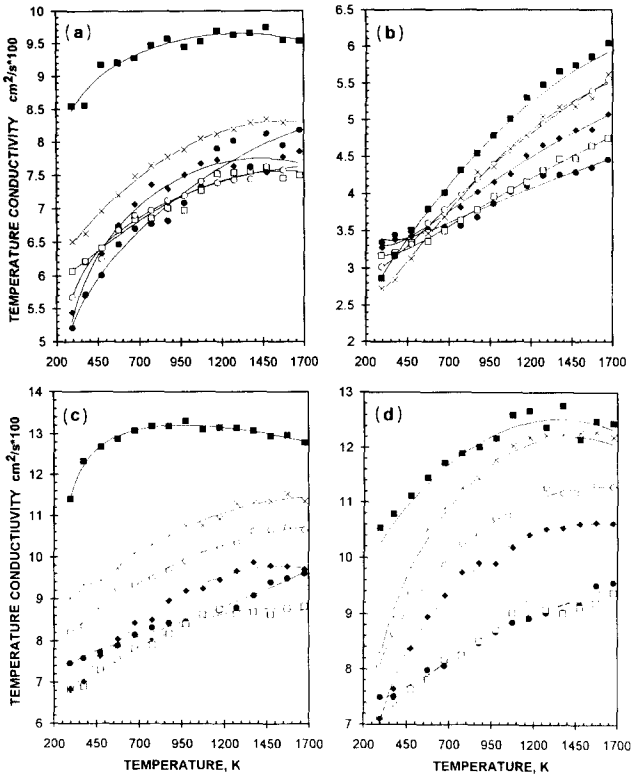

Fig. 10. Temperature diffusivities of IVb carbonitrides as a function of temperature. The coefficients of the polynomials are contained in Table 5. a: ●, Ti 550; □, Ti 541; ♦, Ti 532; ○, Ti 523; ×, Ti 514; ■, Ti 505. b: ●, Ti 450; □, Ti 369; ♦, Ti 2718; ○, Ti 1827; ×, Ti 936; ■, Ti 045. c: ●, Zr 550; □, Zr 541; ♦, Zr 532; ○, Zr 523; ×, Zr 514; ■, Zr 505. d: ●, Hf 550; □, Hf 541; ♦, Hf 532; ○, Hf 523; ×, Hf 514; ■, Hf 505. Compositions of samples are given in Table 2.

work. The temperature conductivity generally increases with increasing nitrogen content (Figs. 10a–10d). A steep increase exists between the nitrogen-richest carbonitrides (the nitrogen-richest carbonitrides studied were practically pure nitrides except for the nitrogen-richest zirconium sample, which, however, showed a similar increase). This increase is less pronounced for $Hf(C_xN_{1-x})_{1.00}$ (Fig. 10d) than for the other two stoichiometric series (Figs. 10a and 10c). The data points were fitted to the polynomial equation

$$\alpha(T)=A+BT+CT^2+DT^{-2} \quad (10^2\ \mathrm{cm^2\ s^{-1}}) \qquad (6)$$

and the results are given in Table 5. Substoichiometric titanium carbonitrides show a deviation from this behaviour at $T \lesssim 500$ K (Fig. 10b). In this region the order in temperature diffusivity is practically reversed as compared with the high temperature values. The lower temperature diffusivity of $Ti(C_xN_{1-x})_{0.82}$ as compared with $Ti(C_xN_{1-x})_{1.00}$ can be explained by a lower number of electrons contributing to the transport process. Obviously the higher the nitrogen content, the more temperature sensitive the temperature diffusivity is.

3.6. Heat conductivity

It is clear that when the temperature diffusivity and heat capacity generally behave similarly with respect to the [C]/([C]+[N]) ratio – increasing with increasing nitrogen content – the heat conductivity also increases with increasing nitrogen content. At small carbon content the temperature conductivity decreases steeply with increasing [C]/([C]+[N]) ratio, which is a similar function to the electrical conductivity at room temperature (Fig. 3). It stems from the behaviour of temperature diffusivity vs. [C]/([C]+[N]) ratio, since the C_p data are approximately linear with [C]/([C]+[N]). The detailed results are presented graphically in Figs. 11a–11d and the coefficients of the polynomial equation

$$k_t(T)=A+BT+CT^2+DT^{-2} \quad (\mathrm{W\ m^{-1}\ K^{-1}}) \qquad (7)$$

are listed in Table 6 (same type of polynomial as for the C_p data fit).

Taylor [13] and Taylor and Morreale [14] report the opposite behaviour with a much higher heat conductivity for TiC than for TiN (see Fig. 11a) and their values for TiC (one sample with free carbon and one with the composition $TiC_{0.95}$) and ZrC (contained in Ref. [15]) are substantially higher than our values for stoichiometric TiC and ZrC, respectively. Their low value for TiN can be attributed largely to the much-lower-than-stoichiometric nitrogen content, which was about [N]/[Ti]=0.79. Indeed, they agree more closely with our values for [N]/[Ti]=0.82; see Fig. 11b (the dis-

Table 5
Coefficients of the polynomial $\alpha(T)=A+BT+CT^2+DT^{-2}$ for the temperature diffusivity data fit (see Figs. 10a–10d)

[C]/([C]+[N])	A	$B\times10^3$	$C\times10^7$	$D/10^4$
$Ti(C_xN_{1-x})$				
0.01	8.49	1.84	−7.177	−4.276
0.21	5.61	3.44	−10.94	−0.489
0.40	5.96	1.84	−4.938	−6.508
0.60	5.52	3.24	−11.53	−9.016
0.79	5.14	3.02	−9.494	1.145
0.99	4.97	3.03	−6.603	−4.805
$Ti(C_xN_{1-x})_{0.82}$				
0.00	1.83	3.85	−8.045	0.0602
0.20	1.41	3.94	−8.973	1.809
0.40	1.97	2.97	−5.051	1.922
0.60	2.32	2.20	−3.422	3.210
0.80	2.36	1.79	−2.219	2.698
1.00	2.71	1.33	−1.720	2.694
$Zr(C_xN_{1-x})$				
0.11	13.37	0.447	−4.403	−17.323
0.25	7.69	4.25	−11.960	1.886
0.43	7.37	3.63	−9.464	−1.397
0.61	5.18	5.98	−19.414	0.169
0.79	5.30	4.67	−15.680	2.193
0.96	7.53	0.69	3.468	−2.938
$Hf(C_xN_{1-x})$				
0.05	9.05	5.18	−19.205	−1.181
0.21	7.72	6.50	−23.210	−10.292
0.40	7.50	4.82	−15.223	−6.080
0.59	6.91	4.93	−16.189	−10.161
0.78	5.92	4.10	−12.638	0.940
0.96	6.49	2.77	−5.186	2.060

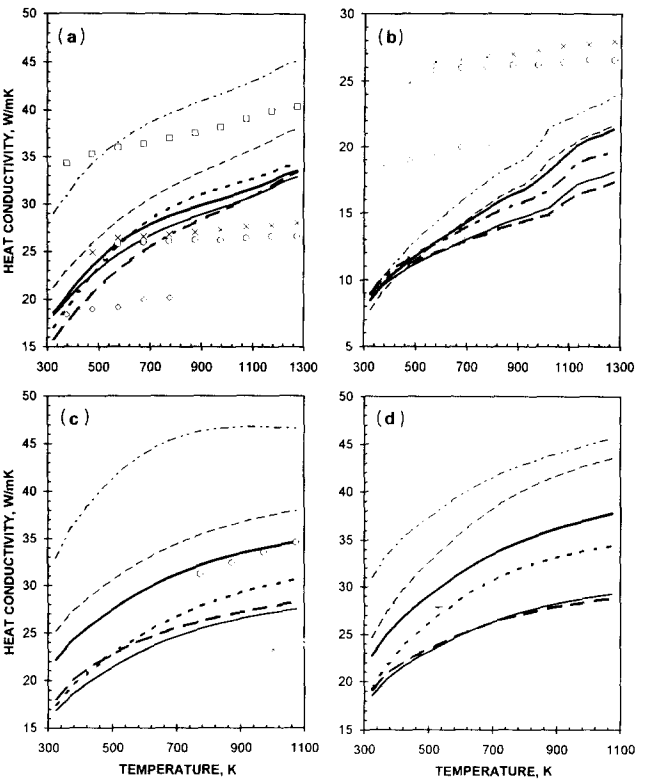

Fig. 11. Heat conductivities of IVb carbonitrides as a function of temperature (for compositions of samples see Table 2). The coefficients for the polynomials are given in Table 6. The discontinuity at around 1000 K observed for the substoichiometric titanium carbonitrides is an intrinsic property due to a phase transformation (see Figs. 8 and 9). a: – – –, Ti 550; —, Ti 541; - - - - -, Ti 532; —, Ti 523; – – – –, Ti 514; - - - - - -, Ti 505; □, TiC [13]; ◇, $TiC_{0.9}$ [14]; ○, $TiN_{0.8}$ [14]; ×, $TiN_{0.8}$ [14]. b: – – –, Ti 450; —, Ti 369; - - - - -, Ti 2718; —, Ti 1827; – – – –, Ti 936; - - - - - -, Ti 045; ◇, $TiC_{0.9}$ [14]; ○, $TiN_{0.8}$ [14]; ×, $TiN_{0.8}$ [14]. c: – – –, Zr 550; —, Zr 541; - - - - -, Zr 532; —, Zr 523; – – – –, Zr 514; - - - - - -, Zr 505; ○, ZrC [15]; ×, ZrC [46] (extrapolated). d: – – –, Hf 550; —, Hf 541; - - - - -, Hf 532; —, Hf 523; – – – –, Hf 514; - - - - - -, Hf 505.

continuities in the heat conductivities at around 980 K could not be detected by Taylor and Morreale [14], possibly because they did not use C_p data to calculate the heat conductivity at $T>880$ K). Similar arguments of composition cannot, however, be applied to the differences relative to our values for TiC and ZrC, since their samples correspond closely in composition to ours. Grossman [46] made thermal conductivity measurements on ZrC at 1400–2600 K and found values about 30% lower than those of Taylor [15] and in better agreement with the values of the present study (Fig. 11b).

3.7. Colour

The reflectance curves for the carbonitride series are presented in Figs. 12a–12d. For the nitrides a distinct minimum in the reflectance curves in the blue region could be observed, indicative of a yellow appearance of the nitrides which is well known from the literature [21–26]. Upon introduction of carbon this minimum shifts towards higher wavelengths and becomes weaker. This was also found by Knosp and Goretzki [26] for titanium and zirconium carbonitrides. The reflectance behaviour they observed is in full agreement with our present findings. The wavelength shift corresponds to a conversion of colour appearance towards violet. This colour change from yellow through violet to grey is shifted towards higher carbon contents the higher the atomic number of the transition metal is. Thus for the same composition the wavelength minima in the reflection curve have the order $\lambda_{min}(Hf(C_xN_{1-x})_{1-y})<\lambda_{min}(Zr(C_xN_{1-x})_{1-y})<\lambda_{min}(Ti(C_xN_{1-x})_{1-y})$. For instance, the position of the minimum in the reflectance curves for $Me(C_{0.6}N_{0.4})$ carbonitrides is at 520, 570 and 640 nm respectively and $Hf(C_{0.6}N_{0.4})$ still appears to be faintly coloured, definitely more so than $Zr(C_{0.6}N_{0.4})$, while $Ti(C_{0.6}N_{0.4})$ is already grey. The substoichiometric carbonitrides show almost linear reflectance curves without a pronounced minimum in any spectral region (Fig. 12b), which is the reason for their uncoloured grey appearance.

Table 6
Coefficients of the polynomial $k(T)=A+BT+CT^2+DT^{-2}$ for the heat conductivity data fit for the stoichiometric samples (see Figs. 11a, 11c and 11d). The data of $Ti(C_xN_{1-x})_{0.82}$ were not fitted owing to the discontinuity in C_p

[C]/([C]+[N])	A	$B\times10^3$	$C\times10^6$	$D/10^5$
$Ti(C_xN_{1-x})$				
0.01	33.453	9.679	−0.147	−8.1666
0.21	19.842	19.090	−3.708	−4.7049
0.40	22.105	11.328	−1.718	−7.6324
0.60	13.496	29.968	−10.754	−5.4960
0.79	20.098	11.630	−1.143	−5.8377
0.99	15.887	16.740	−2.281	−5.7473
$Zr(C_xN_{1-x})$				
0.11	48.209	1.799	−1.616	−17.0671
0.25	25.067	19.029	−5.976	−5.7869
0.43	22.761	17.266	−5.262	−6.0278
0.61	15.031	23.285	−7.725	−4.5450
0.79	16.394	16.873	−5.644	−4.6822
0.96	22.110	7.224	−0.804	−6.6003
$Hf(C_xN_{1-x})$				
0.05	34.379	14.250	−2.694	−8.1179
0.21	21.727	33.683	−11.692	−7.1762
0.40	21.273	24.601	−8.006	−5.9277
0.59	19.253	24.543	−8.981	−7.3301
0.78	17.392	18.476	−6.517	−4.3039
0.96	19.484	14.264	−4.788	−4.6140

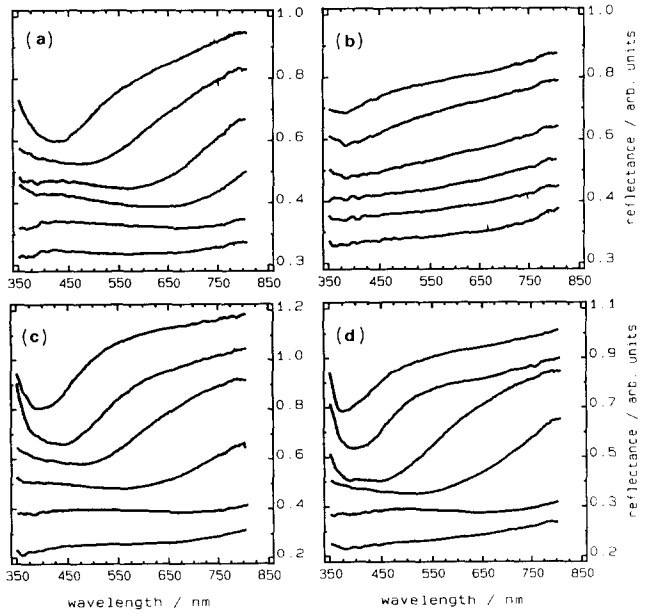

Fig. 12. Reflectance of stoichiometric IVb carbonitrides and $Ti(C_xN_{1-x})_{0.82}$ as a function of [C]/([C]+[N]) ratio. A shift in the y axes between each curve was introduced for the graphical representation (the reflectances at around 800 nm are very similar). a: $Ti(C_xN_{1-x})_{1.00}$, from top to bottom Ti 505, Ti 514, Ti 523, Ti 532, Ti 541, Ti 550. b: $Ti(C_xN_{1-x})_{0.82}$, from top to bottom Ti 045, Ti 936, Ti 1827, Ti 2718, Ti 369, Ti 450. c: $Zr(C_xN_{1-x})_{1.00}$, from top to bottom Zr 505, Zr 514, Zr 523, Zr 532, Zr 541, Zr 550. d: $Hf(C_xN_{1-x})_{1.00}$, from top to bottom Hf 505, Hf 514, Hf 523, Hf 532, Hf 541, Hf 550. For compositions of samples see Table 2.

Acknowledgments

This work was sponsored by the Jubiläumsfonds der Oesterreichischen Nationalbank under Project 3729. Support through the French–Austrian research contract, Project A11, is also gratefully acknowledged. Hafnium and zirconium sponges were supplied by Teledyne Wah Chang, USA, for which the authors express their appreciation. Mrs C. Jelinek helped with the preparation of the manuscript.

References

[1] P. Ettmayer, *Ann. Rev. Mater. Sci., 19* (1989) 145.
[2] E.K. Storms, *The Refractory Carbides,* Academic, New York, 1968.
[3] L.E. Toth, *Transition Metal Carbides and Nitrides,* Academic, New York, 1971.
[4] P. Ettmayer and W. Lengauer, Carbides: transition metal solid state chemistry, in *Encyclopedia of Inorganic Chemistry,* Wiley, New York, 1994, in press.
[5] P. Ettmayer and W. Lengauer, Nitrides: transition metal solid state chemistry, in *Encyclopedia of Inorganic Chemistry,* Wiley, New York, 1994, in press.
[6] P. Ettmayer and W. Lengauer, Nitrides, in *Ullmann's Encyclopedia of Industrial Chemistry,* Vol. 17, Verlag Chemie, Weinheim, 1991, p. 341.
[7] S. Binder, W. Lengauer, P. Ettmayer, J. Bauer, J. Debuigne and M. Bohn, *J. Alloys Comp., 217* (1995) 128.
[8] G.D. Bogomolov, G.P. Shveikin, S.I. Alyamovskii, Y.G. Zainulin and V.D. Lyubimov, *Izv. Akad. Nauk SSSR, Neorg. Mater., 7* (1971) 67.
[9] R. Kieffer, W. Wruß, K. Constant and H. Habermann, *Monatsh. Chem., 106* (1975) 1349.
[10] F. Binder, *Radex Rundschau, 4* (1975) 531.
[11] E. Barbier and F. Thevenot, *J. Mater. Sci., 27* (1992) 2383.
[12] B. Schulz, *Nuclear Research Centre Karlsruhe, KfK Rep. 2826B,* 1978, p. 113.
[13] R.E. Taylor, *J. Am. Ceram. Soc., 44* (1961) 525.
[14] R.E. Taylor and J. Morreale, *J. Am. Ceram. Soc., 47* (1964) 69.
[15] R.E. Taylor, *J. Am. Ceram. Soc., 45* (1962) 353.
[16] W.S. Williams, *J. Am. Ceram. Soc., 49* (1966) 156.
[17] W.S. Williams, in R. Freer (ed.), *The Physics and Chemistry of Carbides, Borides and Nitrides,* Kluwer, Dordrecht, 1991, p. 625.
[18] A.G. Turchanin, S.A. Babenko and I.I. Bilyk, *Izv. Akad. Nauk SSSR, Neorg. Mater., 20* (1984) 1511.
[19] A.G. Turchanin, S.A. Babenko and V.S. Polishchuk, *Zh. Fiz. Khim., 56* (1982) 41.
[20] A.G. Turchanin and S.A. Babenko, *Izv. Akad. Nauk SSSR, Neorg. Mater., 21* (1985) 1325.
[21] B. Karlsson, R.P. Shimshock, B.O. Seraphin and J.C. Haygarth *Solar Energy Mater., 7* (1983) 401.
[22] A. Schlegl, P. Wachter, J.J. Nickl and H. Lingg, *J. Phys. C Solid State Phys., 10* (1977) 4889.
[23] A.J. Perry, M. Georgson and C.G. Ribbing, *J. Vac. Sci. Technol A, 4* (1986) 2674.
[24] H.G. Tompkins, R. Gregory and B. Boeck, *Surf. Interface Anal. 17* (1991) 22.
[25] W. Lengauer, H. Böhm and P. Ettmayer, *Mikrochim. Acta,* in press.
[26] H. Knosp and H. Goretzki, *Z. Metallk., 60* (1969) 587.

[27] R. Täubler, S. Binder, M. Groschner, W. Lengauer and P. Ettmayer, *Mikrochim. Acta I, 107* (1992) 337.
[28] K.D. Maglic, A. Cezairliyan and V.E. Peletsky (eds.), *Compendium of Thermophysical Property Measurement Methods,* Vol. 1, *Survey of Measurement Techniques,* Plenum, New York, 1984, p. 305.
[29] L.M. Clark and R.E. Taylor, *J. Appl. Phys., 46* (1975) 2.
[30] K. Aigner, W. Lengauer, D. Rafaja and P. Ettmayer, *J. Alloys Comp., 215* (1994) 121.
[31] G. Ondracek, *Rev. Powder Metall. Phys. Ceram., 3*(3–4) (1987) 205.
[32] H. Holleck and H. Schweitzer, *Nuclear Research Centre Karlsruhe, KfK Rep. Ext. 6/74-2,* 1974, p. 47.
[33] J.-L. Chermant, P. Delavignette and A. Deschanvres, *J. Less-Common Met., 21* (1970) 89.
[34] W. Lengauer, *J. Alloys Comp., 186* (1992) 293.
[35] B. Naylor, *J. Am. Ceram. Soc., 68* (1946) 370.
[36] O. Kubaschewski, in K.L. Komarek (ed.), *Titanium, Physicochemical Properties of its Compounds and Alloys, Atomic Energy Review,* Spec. Issue 9, International Atomic Energy Agency, Vienna, 1983.
[37] A.G. Turchanin, *Izv. Akad. Nauk SSSR, Neorg. Mater., 22* (1986) 1299.
[38] C.B. Alcock, K.T. Jacon and S. Zador, in O. Kubaschewski (ed.), *Zirconium, Physicochemical Properties of Its Compounds and Alloys, Atomic Energy Review,* Spec. Issue 6, International Atomic Energy Agency, Vienna, 1976, p. 7.
[39] H.L. Schick, *Thermodynamics of Certain Refractory Compounds,* Vol. II, Academic, New York, 1966, Sect. 7–9.
[40] R. Hultgren, P.R. Desai, D.T. Hawkins, M. Gleiser and K.K. Kelley, *Selected Values of Thermodynamic Properties of Binary Alloys,* ASM, Metals Park, OH, 1973.
[41] J.P. Coughlin and E.G. King, *J. Am. Chem. Soc., 72* (1950) 2262.
[42] M.P. Arbuzov, S.Y. Golub and B.V. Khaenko, *Izv. Akad. Nauk SSSR, Neorg. Mater., 14* (1978) 1442.
[43] G. Lobier and J.P. Marcon, *C.R. Acad. Sci. Paris C, 268* (1969) 1132.
[44] E. Etchessahar, Y.-U. Sohn, M. Harmelin and J. Debuigne, *J. Less-Common Met., 167* (1991) 261.
[45] W. Lengauer, *J. Alloys Comp., 179* (1992) 289.
[46] L.N. Grossman, *J. Am. Ceram. Soc., 48* (1965) 236.